

# Bunch Compression and CSR Study in ASTA

DHRUV KEDAR

Department of Physics, University of Chicago, Chicago, IL, 60637

TANAJI SEN

Accelerator Physics Center, Fermi National Accelerator Laboratory, Batavia, IL, 60510

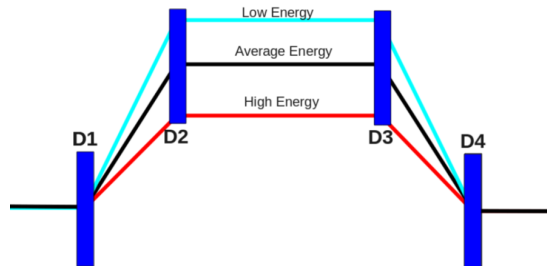
## Abstract

*Bunch compression through two chicanes will be explored in Fermilab's new Advanced Superconducting Test Accelerator test facility. Partial compression of a 40MeV bunch and its acceleration to higher energies before full compression offers advantages in maximization of peak current and minimization of bunch length. Additional effects due to coherent synchrotron radiation (CSR) quickly become apparent at these energies and introduce nonlinearities in the longitudinal phase space that are less than optimal for acceleration to high energies. We show that two-stage compression offers several advantages in this area if the bunch is initially partially compressed to weaken the propagation of CSR distortions incurred in the first bunch compressor BC1. This results in a higher peak current that we could obtain if we sought full compression through the first chicane.*

## I. INTRODUCTION

The Advanced Superconducting Test Accelerator (ASTA) facility at Fermilab is proposed as a state-of-art electron linear accelerator using superconducting RF technology. Intended as a test facility for developing SRF cryomodules, it is ultimately purposed with studying the design of the International Linear Collider (ILC) components. The facility is therefore designed and equipped for generating electron beams with ILC parameters and accelerating them to energies in the range of 750 MeV - 1 GeV. Illustrated in Fig.1, the low-energy photoinjector beamline generates a 4.5 MeV electron bunch from 1.3 GHz photocathode gun, and accelerates it to 40 MeV within two 1.3 GHz 9-cell superconducting RF cavities (CAV1 and CAV2). A third higher frequency 3.9 GHz cavity is placed after CAV2 for the purpose of linearizing the longitudinal phase space for passage through a four dipole bunch compressor (BC1). BC1 takes advantage of the bunch's correlated energy spread to bend particles of different momentum through different path lengths where they recombine as a smaller, more compact bunch (see Fig.2). [2]

ASTA plans to use two magnetic chicanes to achieve full bunch compression. After BC1, electron bunches will be accelerated to their maximum energy through a series of SRF cryomodules, each containing eight 9-cell cavities with a 25 MV/m average accelerating gradient. Beyond this section lies the final magnetic compressor, where full compression is reached. Unlike BC1 which consists of 0.2m long dipoles with bend angles of 18 degrees, BC2 is expected to be weaker, with dipole bend angles of less than 10 degrees. This paper presents a study of different compression schemes and optimization of the cavity settings for maximum longitudinal bunch compression.



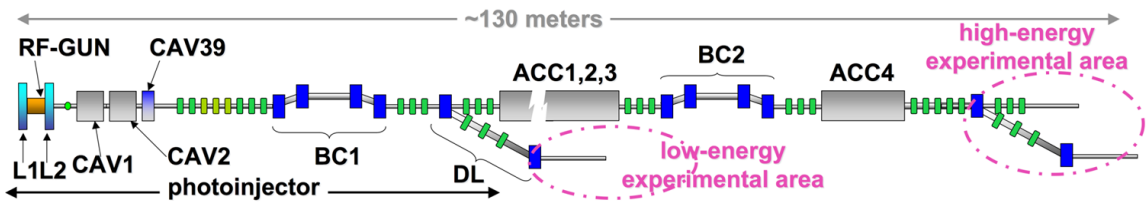


Figure 1: ASTA Beamline

Figure 2: The dipole magnetic fields bend the particle trajectories, causing those with higher momenta to traverse a shorter distance. At these energies, velocity spreads are negligible due to relativistic effects

Additionally we consider coherent synchrotron radiation (CSR) effects from acceleration through the bunch compressor dipoles. Radial acceleration of charged particles causes them to emit photon radiation, but at relativistic velocities this radiation becomes coherent and affects the position of particles within the same bunch. As the tail of the bunch passes through the dipoles, coherent radiation interacts with the bunch head, causing emittance growth, energy spread, and a decrease in peak current. This results in unwanted geometric distortions in the longitudinal phase space after compression. [4]

Simulations of longitudinal beam dynamics are studied with the ELEGANT code (Electron Generation and Tracking) developed at Argonne National Lab. Beam dynamics can be modeled with added effects of space charge and CSR but space charge effects can only be implemented in drift regions, ignoring them in RF cavity elements and dipoles. Since we predict SC effects to be large in the beamline up to BC1 and we cannot accurately study it in RF cavities 1, 2, and 39, we ignore it entirely. Thus, this paper deals with CSR effects in the 1D dynamics from the end of the photoinjector to the end of the second bunch compressor.

We consider an initial bunch of Gaussian distribution with ILC parameters. Previous studies with Elegant have indicated that a minimum of 40000 particles is needed to produce an accurate simulation of CSR effects in the

bunch compressor dipoles. [3]

Parameter	Value
Particles	40000
$\sigma_s$	2.4 mm
$\frac{\delta p}{p}$	0.0023
Charge	3.2 nC

Table 1: Initial Bunch Parameters

## II. OPTIMIZATION PROCEDURE

Optimization of beam elements is calculated incrementally, by sequentially optimizing cavities without any dispersive effects, and then adjusting phases and voltages with the inclusion of CSR.

### 2.1 CAV1

CAV1 is operated on crest (Elegant uses a convention of  $\phi = 90$  for on-crest - this phase gives the maximum acceleration through the RF cavity) in order to deliver maximum energy to the accelerated bunch. With an average accelerating gradient of 22MeV/m for the  $\sim 1$ m RF cavity and the initial 4.5MeV delivered to the bunch in the photoinjector, total energy after exit of CAV1 should be 26.5MeV.

### 2.2 CAV2

Rotation of the phase space in the bunch compressor is accomplished by introducing a second RF cavity after CAV1 and accelerating particles off-crest. Adjusting the cavity so that the bunch crosses at a nonzero phase imparts different energies to the head and tail, in turn creating a larger energy spread. We choose a

phase where particles at the tail of the bunch are increased in energy to take a shorter path through the chicane and consequently move to the front of the bunch. The energy gained by a particle at position  $z$  in the bunch when passing through the cavity is represented by

$$E(z) = eV \cos(kz + \phi) \quad (1)$$

where  $V$  is the peak voltage,  $k$  is the wave number and  $\phi$  is the initial phase.

Sinusoidal RF acceleration introduces nonlinear effects to the phase space. Acceleration at peak RF from CAV1 and CAV results in a C-shaped phase ellipse, and its rotation through the chicane results in poor bunch compression. The effects can be countered by introducing an energy-position correlation by accelerating particles on the falling edge of the sinusoid wave. Nonlinearities of the energy chirp can be removed by manipulating the Fourier sum of RF voltages to result in an energy gain that is nearly linear in  $z$ . A linearized phase ellipse, when compressed, will yield the highest peak current and smallest bunch size. We accomplish this by approximating the energy-position correlation through a Taylor expansion, and introducing cavities with off-crest chirps to match and eliminate higher order terms. Defining the CAV2 chirp as  $h_1$ ,

$$E(z) = E_0 \delta E(z) \quad (2)$$

Where

$$\delta E(z) = 1 + h_1 z + O(z^3) \quad (3)$$

We find that we match the chirp of CAV2 to the first order approximation for  $E(z)$ . It turns out that maximum compression occurs when  $h_1 = R_{56}^{-1}$  where  $R_{56}$  is the compression factor of the first chicane. With CAV1 operated on crest, the first order Taylor expansion yields

$$E(z) = E_0 - [eV_2 k_2 \sin(\phi_2)]z + O(z^2) \quad (4)$$

With the maximum compression condition, the required off-crest phase can be calculated analytically

$$\frac{1}{R_{56}} = \frac{eV_2}{E_0} k_2 \sin \phi_2 \quad (5)$$

So

$$\phi_2 = \sin^{-1} \left[ \frac{E_0}{eV_2 k_2} \frac{1}{|R_{56}|} \right] \quad (6)$$

### 2.3 Linearization and CAV39

The higher order terms of the energy expansion are not negligible, and failing to correct for them results in a quadratic droop in the phase space of the bunch after CAV2. Nonlinearities are apparent in the pre-compression phase space and are intensified when passing through the first chicane. Thus, we use a third higher harmonic cavity to remove the quadratic dependence. The third SRF module (CAV39) operates at an effective gradient of 5MV/m, a frequency 3.9GHz, and is consequently one-third the length of the first two cavities. The addition of an accelerating element to the beamline complicates the total RF voltage as there are now contributions from the higher harmonic, but it is now possible to eliminate the effects of the  $z^2$  term. From the second order expansion, we set the quadratic term

$$\frac{1}{2} [eV_1 k_1^2 \cos \phi_1 + eV_2 k_2^2 \cos \phi_2 + eV_{39} k_{39}^2 \cos \phi_{39}] z^2 = 0 \quad (7)$$

Simplifying to the case where CAV2 is on-crest,

$$[eV_1 k_1^2 + eV_2 k_2^2 + eV_{39} k_{39}^2 \cos \phi_{39}] = 0 \quad (8)$$

We find

$$\phi_{39} = \pi \quad (9)$$

$$V_3 = \frac{V_1 k_1^2 + V_2 k_2^2}{k_3^2} \quad (10)$$

An off-crest phase in CAV2 requires a correction  $\delta \phi_3$ , calculated by substituting in the phase dependent term in the second order expansion

$$V_1 k_1^2 + V_2 k_2^2 \cos \phi_2 + V_{39} k_{39}^2 \cos \phi_{39} = 0 \quad (11)$$

With the inclusion of the phase deviation, we find for CAV39

$$\phi_{39,T} = \pi + \cos^{-1} \left[ \frac{V_1 + V_2 \cos \phi_2}{V_1 + V_2} \right] \quad (12)$$

A dependence on on CAV39 phase in the linear  $z$  term introduces an additional deviation  $\delta\phi_2$  given by

$$\delta\phi_2 = -\frac{k_1 V_1 + k_2 V_2}{k_3 V_2 \cos\phi_2} \left[ 1 - \left( \frac{V_1 + V_2 \cos\phi_2}{V_1 + V_2} \right)^2 \right]^{1/2} \quad (13)$$

So

$$\phi_{2,T} = \phi_2 + \delta\phi_2 \quad (14)$$

With the inclusion of CAV39, it should be possible to have an entirely linear, vertical phase ellipse after rotation through the first bunch compressor.

## 2.4 BC1 and CSR

As the  $R_{56}$  of the first bunch compressor (BC1) remains fixed, optimization can only occur through variation of the cavity phases and voltages. Cavities one and two are operated at this average gradients to ensure maximum bunch acceleration, though  $V_{39}$  can be analytically determined as shown above. Our optimization procedure follows that outlined above. We first consider the beamline consisting solely of accelerating elements CAV1, CAV2, and BC1. Variation of CAV2 phase that yields peak current and minimal bunch size is the optimal value and is expected to match the analytic value. The beamline is then modified to include CAV39 before BC1 and all cavities are run on crest for optimization of  $V_{39}$  (note that CAV39 is a decelerating cavity). As  $k_{39} = 3k_1 = 3k_2$ , the correct  $V_{39}$  should result in a loss of  $\frac{1}{9}$ th the energy after acceleration through CAV2. Finally, CAV2 is run at  $\phi_{2,T}$  and we scan around  $\phi_{39,T}$  to find the optimal phase.

Inclusion of CSR effects requires modification of the Elegant lattice file, where head-tail interactions are modeled as a series of radiation kicks within the dipoles. CSR deviations are determined numerically through the process detailed above. Optimal phases can be expected to shift closer to on-crest as more energy is required to account for the loss through synchrotron radiation.

## 2.5 Two-stage Compression

Two stage bunch compression offers several advantages over the single full compression case. Full compression from BC1 introduces a CSR induced momentum spread and phase space nonlinearities that must be dealt with through the rest of the beamline. With two stage compression, CAV2 and CAV39 can be operated off their optimal phases closer to crest so that the phase space is linear, but the bunch is not fully compressed as it passes through BC1. CSR effects from the bunch rotation introduce an energy spread and nonlinearities to the bunch, but since compression is not maximal the effects are much less destructive than in the full compression case. After BC1 the first accelerating cryomodule (CM1, additional cryomodules can be added in succession with the rest on crest) can be operated off crest to again linearize the phase space; the rotation through BC2 then fully compresses the bunch with less distortion from the CSR since the dipoles of the second compressor can be of a lower bending angle. We have the added freedom of having a tuneable  $R_{56}$  for the second compressor, allowing us a second optimization parameter for the latter half of compression. With this, we can match an optimal  $R_{56}$  to each off-crest phase of the accelerating cryomodule and scan for the combination that gives us optimal bunch compression - figures of merit for the optimal phase- $R_{56}$  combination are peak current, RMS length, energy spread, and bunch energy. Maximum compression through BC1 is suggested to be  $800\mu m$ , and BC2 is expected to have a lower bend angle of  $5 - 10^\circ$ . However, the optimal  $R_{56}$  of BC2 for given CM1 phase can be approximated analytically with the same method for setting the phase of CAV2. A small-angle approximation for the compression factor yields

$$R_{56} \approx -2\theta^2 \left[ \frac{2}{3} L_D + L_{12} \right] \quad (15)$$

For dipole length  $L_D$  and separation  $L_{12}$ . Substitution into the  $\phi_2$  expression establishes a relation [1] between bend angle and cryomod-

ule phase

$$\phi_{CM} = \sin^{-1} \left[ \frac{E_0}{eV_{CM}k_{CM}} \left( \frac{1}{2\theta^2 \left[ \frac{2}{3}L_D + L_{12} \right]} \right) \right] \quad (16)$$

Scanning across different bend angles presents an associated  $\phi_{CM}$  which we then vary separately to find the optimal compression phase. Different  $R_{56} - \phi_{CM}$  combinations can be considered for a preferred set of final bunch parameters.

### III. RESULTS

We first study the relative effects of the CAV39 inclusion in the beamline without CSR to ensure we are properly linearizing the longitudinal phase space.

#### 3.1 Full-stage Compression

The beam element parameters we use are specified in Table 2. From (6) we expect an off-crest CAV2 phase of 18 degrees and Elegant simulations with just CAV1 and CAV2 before the first compressor indeed suggest an optimal  $\phi_2$  of 18 degrees. As illustrated in Fig. 3, phase space before the first compressor is not entirely linear, and the slight quadratic curvature is maintained and amplified when passing through BC1.

Element	Value
CAV1 Voltage	22MV
CAV1 Frequency	1.3 GHz
CAV2 Voltage	22MV
CAV2 Frequency	1.3 GHz
CAV39 Voltage	0.0023
CAV39 Frequency	3.9 GHz
BC1 Bend Angle	18°
BC1 Dipole Length	0.301 m
BC1 $R_{56}$	0.192

Table 2: Parameters for beamline elements for full-compression case

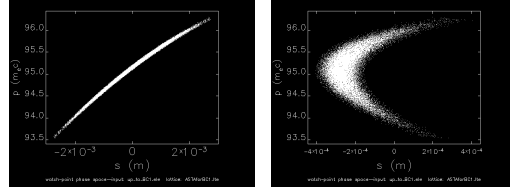


Figure 3: Bunch phase space without the inclusion of CAV39 in the beamline. Images above display phase space before and after BC1

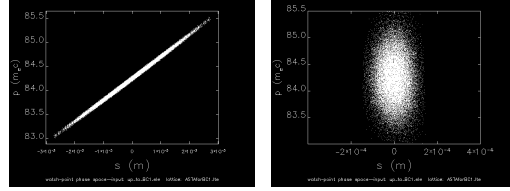


Figure 4: Bunch phase space with CAV39 in the beamline. From left to right, phase space before and after BC1. Note that with linearization of the LPS before BC1, there are no distortions after compression

Addition of the 3.9 GHz cavity removes the dominant higher order effects, visible in Fig.4. After CAV39, we see a removal of the quadratic droop at the optimal phases of  $\phi_{2,T} = 64.5$ ,  $\phi_{39,T} = 265$  degrees. These closely match our analytical values of 64.8 and 264 degrees for the respective CAV2 and CAV39 phases.

We are also able to further compress the bunch from a previous rms length of  $91 \mu\text{m}$  to  $49 \mu\text{m}$ , giving us a higher peak current of over 8000 A. For setting  $V_{39}$ , we obtain an analytical expression relating it to the voltages of the two accelerating cavities in eq. (10). With RF frequencies  $k_1$  and  $k_2$  of 1.3 GHz, we expect a CAV39 voltage of 5.39 MV. We check this numerically as well: since CAV39 decelerates the bunch, we should expect its energy to drop by  $\frac{1}{9}$ th as it passes through, and we find that  $V_{39} = 5.38 \text{ MV}$ .

Adding CSR effects we immediately see distortions in bunch distribution, particularly apparent in the vicinity of the head. RMS bunch size grows to  $432 \mu\text{m}$  with a decrease in peak current to less than 900 A. However, several of the nonlinearities can be approximated by quadratic corrections, suggesting we make use of CAV39. Optimization with regards to peak

current yields new bunch parameters of  $\phi_{2,T} = 66^\circ$ ,  $\phi_{39,T} = 266.8$ , and  $V_{39} = 5.38$  MV (comparison of cavity settings are below in table 3). CAV2 phase expectedly moves closer to crest as we account for the energy loss due to synchrotron radiation.

Parameter	CSR off	CSR on
$\phi_2$	$64.5^\circ$	$66.0^\circ$
$\phi_{39}$	$265.0^\circ$	$266.8^\circ$
$V_{39}$	5.38 MV	5.38 MV

Table 3: Full compression through BC1

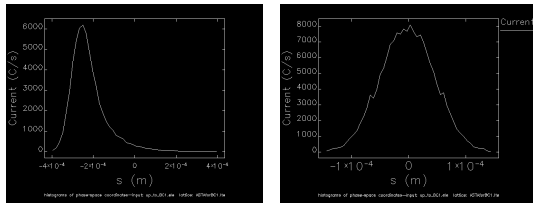


Figure 5: Current profile without and with CAV39. With the higher frequency cavity, the profile's peak occurs at the center of the bunch rather than the head.

### 3.2 Two-stage Compression

For two stage compression, it is recommended that bunch length after BC1 be at a maximum of 800 microns. [5] The necessary settings for optimization at this length are  $\phi_{2,T} = 73$  degrees,  $\phi_{39,T} = 267$  degrees, and  $V_{39} = 5.15$  MV, yielding a peak current of 595 A with CSR included. Note that there can be several different parameter configurations that generate an 800 micron bunch; since this is the only limitation, we choose cavity settings that impart the best shape to the phase space after BC1 for acceleration through the rest of beamline. Since CSR in BC2 will heavily distort the bunch, the post-BC1 bunch is chosen to have a heavier distribution towards the tail.

Optimization to full compression through BC2 has the added option of altering the chicane's  $R_{56}$ . Using a constant dipole length 0.5 m, we can vary the bend angle between reasonable values of 5 and 15 degrees. For optimization alongside the cryomodule phase, we instead choose to vary  $\phi_{CM}$  between 50 and

80 degrees (90 being on-crest) and scan for the associated dipole angle (the bend angle is varied through modification of each dipole in the chicane and is optimized with respect to the bunch's peak current). Without CSR, the bunch is compressed to less than half the length as in the full compression case, and peak current is significantly higher, in excess of 20 kA. With CSR included in BC2, it is expectedly lower, by a factor of approximately 2, with RMS length increasing by the same amount.

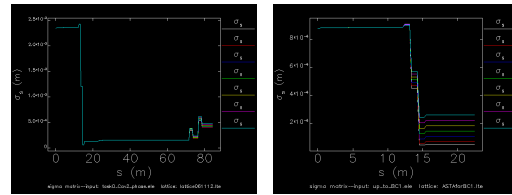


Figure 6: A comparison of RMS length (vertical axis) through the beamline for the full-compression and two-stage compression cases. In full-stage through BC1 (left) passing through the second chicane can do nothing to decrease bunch size and instead lengthens it. For the same phases, two-stage can be more effective.

We additionally consider an initial bunch of a gaussian distribution with a 3ps length (0.9mm) instead of the previous 2.4mm length. 1D longitudinal simulations are carried through the first bunch compressor for the case of full, one-stage compression, and after BC1 the bunch is compressed to a length of 49 microns. However, simulations with CSR effects included along the same beamline identify a possible lower limit on bunch size before it is sent through the chicane. Compression up through the third dipole matches simulations without CSR, reaching a length of 105 microns. At the fourth dipole, CSR effects (on the bunch head) appear to increase RMS size through the fourth dipole to 430 microns. This seems to indicate that there is a minimum bunch length before BC1 required for compression before RMS effects greatly increase RMS size. However, there need to be more simulations done to confirm this.

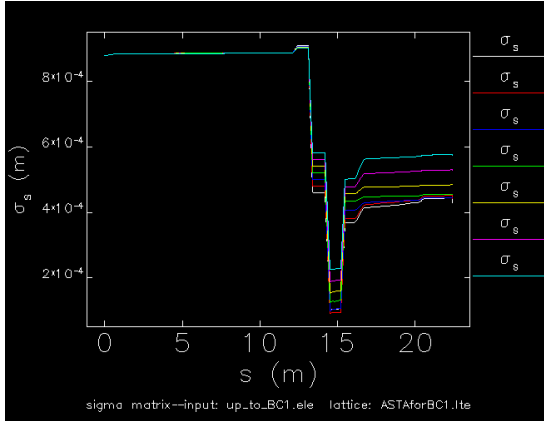


Figure 7: RMS length of the 3ps bunch for a scan of different CM1 phases. After the third dipole in BC2, CSR effects severely increase bunch size.

#### IV. CONCLUSION

So far we have validated the necessity of two-stage compression, and the benefits it offers especially when dealing with CSR. Compared to the scenario of full compression, peak current with CSR increases from 4000A to 11kA; bunch size also necessarily decreases from 190  $\mu\text{m}$  in BC1 to less than 100  $\mu\text{m}$  after BC2. With more CM1 phases simulated, it is trivial to create a contour map of all possible  $R_{56} - \phi_{CM}$  combinations for choosing a bunch with certain characteristics (peak current, RMS length, energy spread, momentum). Unfortunately longitudinal studies do not provide us with all the information necessary for a study of the two-stage compression method. Our best figure of merit is beam brightness which requires

a study of the transverse dynamics. CSR also affects the transverse emittance, so a comprehensive understanding of the radiation effects requires full 6D simulations.

#### V. ACKNOWLEDGEMENTS

I would first and foremost like to thank my mentor Tanaji Sen for his support and patience in guiding me through this project. Additionally, I am grateful for the assistance provided by Chris Prokop and Philippe Piot for using Elegant and developing a procedure for optimization. Finally, I would like to thank Eric Prebys, Linda Spentzouris, and Carol Angarola for the organization of the Lee Teng program and the opportunity to immerse myself in accelerator physics.

#### V. REFERENCES

- [1] T. Sen, "Linearizing Phase Space with Multiple Harmonic Cavity", August 1, 2012
- [2] P. Piot et al., "Beam Dynamics Simulations of the NML Photoinjector at Fermilab" THPD020, Proceedings of IPAC10, Kyoto, Japan.
- [3] C. Prokop, "Simulation Studies of the Low-Energy Bunch Compressor at the Advanced Superconducting Test Accelerator", FNAL-TM-2533-APC.
- [4] C. Prokop, "Performance of Low-Energy Magnetic Bunch Compression for the ASTA Photoinjector at Fermilab", Proceedings of IPAC12, New Orleans, Louisiana, USA
- [5] P. Piot, private communication, 2012

Table 4: Beam characteristics after BC2 without CSR for given cryomodule phases

CM1 Phase	Opt. Angle	Peak I (A)	RMS size ( $\mu$ m)	pCentral	Energy spread
50	6.86	24018	36	397	1.56
55	7.45	23406	34	419	1.34
60	8.05	22064	34	438	1.14
65	8.80	19746	34	454	0.95
70	9.70	18228	36	467	0.78
75	10.95	15161	41	478	0.61
80	12.60	11847	50	486	0.45

Table 5: Beam characteristics after BC2 with CSR for given cryomodule phases

CM1 Phase	Opt. Angle	Peak I (A)	RMS size ( $\mu$ m)	pCentral	Energy spread
50	7.05	11681	38	397	1.98
55	7.65	10337	44	419	1.69
60	8.30	9269	50	438	1.42
65	9.10	7697	59	454	1.17
70	10.10	6465	73	467	0.94
75	11.40	5086	96	478	0.73
80	13.50	3696	146	486	0.53